

Raman phonon anomalies in $Sr(Fe_{1-x}Co_x)_2As_2$

Yanxing Yang(杨彦兴), Hewei Zhang(张鹤巍), and Haizheng Zhuang(庄海正)
Citation: Chin. Phys. B, 2022, 31 (**2**): 027401. DOI: 10.1088/1674-1056/ac0cd6
Journal homepage: http://cpb.iphy.ac.cn; http://iopscience.iop.org/cpb

What follows is a list of articles you may be interested in

Pressure tuning of the anomalous Hall effect in the kagome superconductor CsV_3Sb_5

Fang-Hang Yu(喻芳航), Xi-Kai Wen(温茜凯), Zhi-Gang Gui(桂智刚), Tao Wu(吴涛), Zhenyu Wang(王震宇), Zi-Ji Xiang(项子雾), Jianjun Ying(应剑俊), and Xianhui Chen(陈仙辉)
Chin. Phys. B, 2022, 31 (**1**): 017405. DOI: 10.1088/1674-1056/ac3990

Evolution of superconductivity and charge order in pressurized RbV_3Sb_5

Feng Du(杜锋), Shuaishuai Luo(罗帅帅), Rui Li(李蕊), Brenden R. Ortiz, Ye Chen(陈晔), Stephen D. Wilson, Yu Song(宋宇), and Huiqiu Yuan(袁辉球)
Chin. Phys. B, 2022, 31 (**1**): 017404. DOI: 10.1088/1674-1056/ac4232

Superconductivity in octagraphene

Jun Li(李军) and Dao-Xin Yao(姚道新)
Chin. Phys. B, 2022, 31 (**1**): 017403. DOI: 10.1088/1674-1056/ac40fa

Highly sensitive and stable SERS probes of alternately deposited Ag and Au layers on 3D SiO_2 nanogrids for detection of trace mercury ions

Yi Tian(田毅), Han-Fu Wang(王汉夫), Lan-Qin Yan(闫兰琴), Xian-Feng Zhang(张先锋), Attia Falak, Pei-Pei Chen(陈佩佩), Feng-Liang Dong(董凤良), Lian-Feng Sun(孙连峰), Wei-Guo Chu(褚卫国)
Chin. Phys. B, 2018, 27 (**7**): 077406. DOI: 10.1088/1674-1056/27/7/077406

High-pressure synchrotron x-ray diffraction and Raman spectroscopic study of plumbogummite

Duan Kang(康端), Xiang Wu(巫翔), Guan Yuan(袁冠), Sheng-Xuan Huang(黄圣轩), Jing-Jing Niu(牛菁菁), Jing Gao(高静), Shan Qin(秦善)
Chin. Phys. B, 2018, 27 (**1**): 017402. DOI: 10.1088/1674-1056/27/1/017402

Raman phonon anomalies in $Sr(Fe_{1-x}Co_x)_2As_2$

Yanxing Yang(杨彦兴)[1,2,†], Hewei Zhang(张鹤巍)[2], and Haizheng Zhuang(庄海正)[2]

[1] *School of Physics, Communication and Electronics, Jiangxi Normal University, Nanchang* 330022, *China*
[2] *Department of Physics, New Jersey Institute of Technology, Newark* 07102-1982, *USA*

(Received 20 May 2021; revised manuscript received 18 June 2021; accepted manuscript online 21 June 2021)

Phonon anomalies have been reported in iron-pnictide superconductors indicating a diverse interplay between different orders in the materials. Here, we report Raman scattering measurements on $Sr(Fe_{1-x}Co_x)_2As_2$ ($x = 0$ and $x = 0.04$) single crystals in the B_{2g} symmetry with respect to a 1 Fe unit cell. Upon cooling, we observe a larger split (13 cm^{-1}) of E_g Raman phonon modes pertaining to in-plane Fe and As displacements as the crystals undergo the tetragonal-to-orthorhombic structural phase transition, although a considerable split (9 cm^{-1}) has been reported in $Ba(Fe_{1-x}Co_x)_2As_2$. Furthermore, the splitting of E_g phonon modes is strongly reduced upon doping. We perform an order-parameter analysis revealing a similar doping dependence of E_g phonon splitting as reported in other compounds of the 122 family, indicating these phonon anomalies widely exist in 122 iron-based superconductors and might share the same mechanisms.

Keywords: Raman scattering, superconductor, phonon, phase transition

PACS: 74.25.Gz, 74.25.Kc, 78.30.–j, 74.62.Dh **DOI:** 10.1088/1674-1056/ac0cd6

1. Introduction

The discovery of superconductivity in the LaOFeP compound[1] in 2006 flipped the traditional understanding that Fe is harmful to superconductivity. In 2008, superconductivity was discovered in the compound $LaO_{1-x}F_xFeAs$ with a maximal T_c of 26 K[2] opening up a brand new family of high-T_c superconductors based on iron-arsenide superconducting layers. Since then, superconductivity in a large number of compounds based on iron-arsenide layers has been discovered with T_c up to 56 K.[3–5] On the basis of their chemical formulae, these compounds are mainly referred to as the 1111 family (e.g., LaOFeAs[1]), 122 family (e.g., $BaFe_2As_2$[6]), 111 family (e.g., LiFeAs[7]) and 11 family (e.g., FeSe[8]). The building block shared by all these compounds referred to as the FeAs plane, has been proposed to account for the magnetic and superconducting properties of these systems.[9] Unlike undoped cuprates behaving like Mott insulators, undoped iron-pnictides act like bad metals with a magnetic order of the spin density wave (SDW) at low temperatures. Superconductivity arises from suppressing the magnetic order and structural phase transition upon doping with electrons or holes.[10] More recently, superconductivity is induced in $BaFe_2As_2$ compound without doping or even applying hydrostatic pressure,[11] providing a deeper insight into the interplay between magnetic/structural and superconducting transition.

It is clear that magnetic order and superconducting transition are mutually exclusive, however charge nematicity, SDW and structural transition emerge in almost the same region of the phase diagram, resulting in the ambiguity of these orders at transition points. The evolution of in-plane phonon modes, i.e., E_u and E_g, with temperature have been extensively reported.[12–15] Specifically, upon cooling, a large splitting of E_g Raman phonon modes involving in-plane Fe and As displacements was observed in $Ba(Fe_{1-x}Co_x)_2As_2$ as the crystals undergo the tetragonal-to-orthorhombic transition.[12] Intuitively, doubly degenerate in-plane E_g phonons split for the orthorhombic distortion of lattice during the structural transition. However, such splitting due to the lattice distortion has been suggested to be so tiny that it could not be observed under the current resolutions.[16] Hence, the observed large splitting must be driven by some other degrees of freedom. It has been proposed that charge nematicity is weakly coupled to the lattice,[17,18] thus spin-phonon coupling has been believed to be the driving force of the phonon anomalies.[12] $Sr(Fe_{1-x}Co_x)_2As_2$ compounds exhibit SDW order upon cooling as well as $Ba(Fe_{1-x}Co_x)_2As_2$ with higher transition temperatures, therefore we expect stronger phonon anomalies in $Sr(Fe_{1-x}Co_x)_2As_2$.

Here, we report Raman scattering measurements on $Sr(Fe_{1-x}Co_x)_2As_2$ ($x = 0$ and $x = 0.04$) single crystals with Raman shifts from 9 cm^{-1} up to 400 cm^{-1} in the B_{2g} symmetry with respect to 1 Fe unit cell described elsewhere.[12] Particularly, the two single crystals do not show superconducting transition upon cooling down to 4.2 K, but exhibit magnetic order with Neel temperatures of 203 K and 137 K for $x = 0$ and $x = 0.04$ respectively. Meanwhile, they have tetragonal ($I4/mmm$) symmetry above and orthorhombic ($Fmmm$) symmetry below the Neel temperatures. Upon cooling, We observe a larger splitting of in-plane E_g phonon modes than that of $Ba(Fe_{1-x}Co_x)_2As_2$. Our analysis indicates that the anomalous splitting of in-plane phonon modes is a universal trend towards structural transition in 122 iron-based superconductors

†Corresponding author. E-mail: yy397@njit.edu
© 2022 Chinese Physical Society and IOP Publishing Ltd

and might share the same mechanisms.

2. Experimental details

$Sr(Fe_{1-x}Co_x)_2As_2$ ($x = 0$ and $x = 0.04$) single crystals were grown by a self-flux method. Single crystals of two different compositions ($x = 0$ and $x = 0.04$) were studied. The parent compound $SrFe_2As_2$ was annealed at 700 °C for three weeks and then cooled down to 300 °C. The magnetic transition temperatures (T_N) were determined to be 203 K and 137 K for $x = 0$ and $x = 0.04$ respectively by transport and magnetization measurements, which are consistent with previous studies.[19] Additionally, we notice that there is no detectable discrepancy between the structural and magnetic transition temperatures in $Sr(Fe_{1-x}Co_x)_2As_2$ in contrast to $Ba(Fe_{1-x}Co_x)_2As_2$.[20,21]

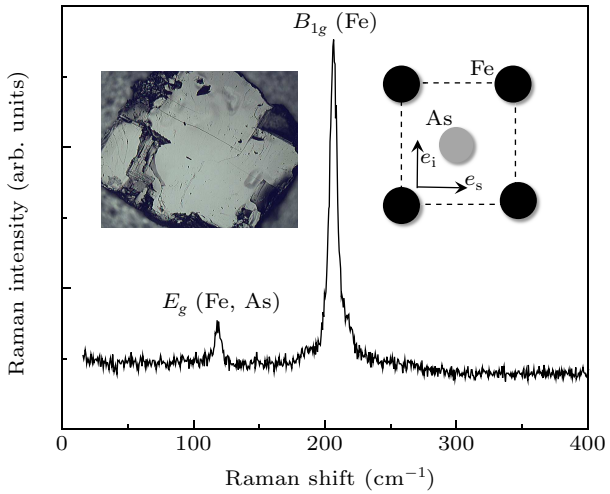


Fig. 1. Raman spectrum of $SrFe_2As_2$ at 315 K in B_{2g} symmetry. Inset: optical image of the freshly cleaved undoped single crystal $SrFe_2As_2$ (left) and geometry of polarization configuration of the B_{2g} symmetry (right).

Single crystals were cleaved under optical microscopy to gain high-quality surfaces (see the inset of Fig. 1) and then sealed in a vacuum of $\sim 10^{-6}$ mbar cooled by a close-cycle refrigerator. Raman scattering experiments were performed using diode pumped solid state laser of $\lambda = 532$ nm and argon-krypton laser of $\lambda = 488$ nm. An incident laser beam of 10 mW was focused on an elliptical spot of dimension 40 μm × 120 μm accounting for a power density of ~ 220 W/cm^2. Reported temperatures were calibrated by taking the laser heating into account. The laser heating was estimated to be 1 K ± 0.2 per mW by monitoring the temperature dependencies of phonon frequencies accounting for 4.5×10^{-2} K $\pm 10^{-2}$ per W/cm^2 in terms of power density. The scattered beam was resolved by a triple stage spectrometer (JY-T64000) equipped with 1800 lines/mm gratings and detected by a liquid nitrogen cooled CCD detector. All the spectra reported here were corrected by eliminating the instrumental response. Polarizations of incident (e_i) and scattered (e_s) lights aligned perpendicular to each other ($e_i \perp e_s$) and along the Fe–Fe bonds (see the inset of Fig. 1) referred to as B_{2g} symmetry in this study.

3. Results and discussion

The imaginary part of the Raman response is derived by $\chi'' \sim [1+n(\omega,T)] \times I$,[22] where I is the Raman intensity measured from experiment, $n(\omega,T)$ the Bose–Einstein distribution and χ'' the imaginary part of Raman response. Figure 1 shows a typical Raman spectrum of $SrFe_2As_2$ in B_{2g} symmetry at room temperature. The crystal has a tetragonal symmetry pertaining to $I4/mmm$ space group above its Neel temperature T_N, wherein the irreducible presentation of the phonon modes is $A_{1g} + B_{1g} + 2E_g + 2A_{2u} + 2E_u$.[23] Specifically, A_{1g} and B_{1g} modes correlate with the displacements of As and Fe along the c axis respectively, and two E_g modes are doubly degenerate involving the displacements of Fe and As in the ab plane for the equivalence of a and c axis in the tetragonal phase. A_{2u} and E_u modes are not Raman-active and will not be discussed here. Since the intensity of the B_{1g} phonon mode is proportional to $\sin^2 2\alpha$ for $e_i \perp e_s$ configuration, where α is the angle between the polarization of incident light e_i and a axis. Noticing that a axis is defined as the diagonal of the 1 Fe unit cell schematized in the Fig. 1, α is 45° for the polarization configuration used here resulting in a maximal Raman intensity of the B_{1g} phonon. In Fig. 1, we notice a sharp peak appearing at 210 cm^{-1}, and the intensity of this peak is proved to be sensitive to the angle α through rotating the sample by a motor equipped in the refrigerator. Therefore, the peak at 210 cm^{-1} is identified as B_{1g} phonon mode (see Fig. 1). Since A_{1g} mode could be only detected by $e_i \parallel e_s$ polarization configuration, we expect there will be no peak corresponding to A_{1g} phonon in this study. The peak at 118 cm^{-1} is indexed to be the Low-frequency E_g phonon (see Fig. 1) since the incident light is polarized along Fe–Fe bond with a finite projection along the c axis as described eleswhere.[12] High-frequency E_g phonon modes seems too weak to be detected here.

Figure 2 shows the evolution of the Raman spectrum ranged from 9 cm^{-1} to 400 cm^{-1} of undoped $SrFe_2As_2$. The spectra are vertically shifted for clearness. The most remarkable feature of the spectra presented in the Fig. 2 is the large splitting of the low-energy E_g phonon across the phase transition. A similar set of spectra is extracted for the $Sr(Fe_{1-x}Co_x)_2As_2$ ($x = 0.04$), wherein the E_g phonon splits at a lower temperature consistent with its lower transition temperature (not shown). In order to gain some insights into the splitting of the E_g phonon mode with temperature, we fit the imaginary part of Raman response around the peaks at 118 cm^{-1} by the superposition of two Lorentzian peaks (see the inset of Fig. 2)

$$\chi'' = \frac{\gamma_1/2\pi}{(\omega_1-\omega)^2+(\gamma_1/2)^2} + \frac{\gamma_2/2\pi}{(\omega_2-\omega)^2+(\gamma_2/2)^2}, \quad (1)$$

where ω_1 and ω_2 are the resonant frequencies of the Lorentz oscillators, γ_1 and γ_2 the line widths. The E_g phonon modes exhibit tiny mean square errors in the fitting, indicating a typical Lorentzian peak of E_g phonons without any detectable asymmetry.

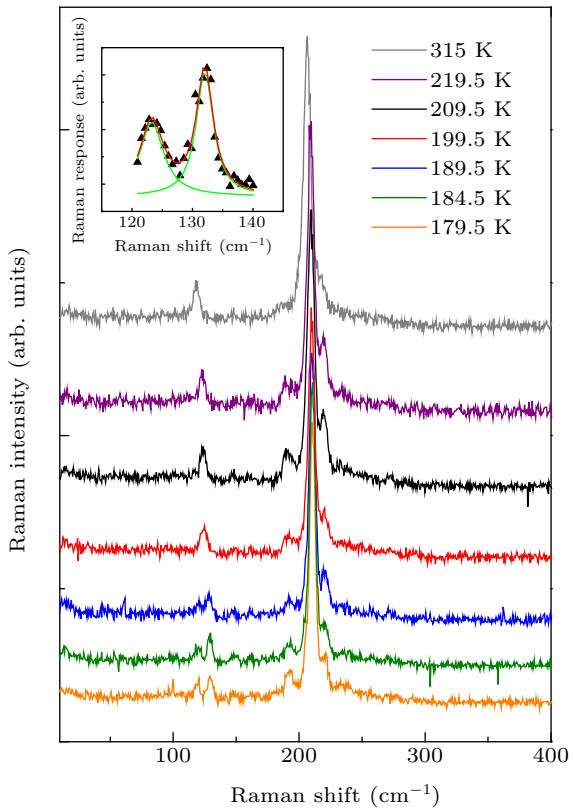


Fig. 2. Evolution with temperature of Raman spectrum of $SrFe_2As_2$ at 315 K in B_{2g} symmetry. Inset: zoom on the splitting E_g phonon modes with fitting curves by two Lorentzian peaks.

The E_g phonon frequencies shown in Fig. 3 are the resonant frequencies fitted by the above equation. The amplitudes of the phonon splitting reach up to 13 cm^{-1} and 8.76 cm^{-1} for $x = 0$ and $x = 0.04$ respectively. As discussed earlier, the amplitude of the in-plane phonon splitting caused by orthorhombic lattice distortion during the structural transition is negligible. Specifically, a simple estimation from the relation between phonon frequency ω and bond length l ($\omega^2 \sim (1/l^3)$)[24] would result in a splitting less than 1 cm^{-1} based on crystallographic data.[25] Remarkably, the largest amplitude of the splitting (13 cm^{-1}) observed in the $Sr(Fe_{1-x}Co_x)_2As_2$ compounds here is much larger than that reported in the $Ba(Fe_{1-x}Co_x)_2As_2$ compounds (9 cm^{-1}).[12] Moreover, the amplitude of the phonon splitting depends on both temperature and doping. Specifically, the amplitudes increase upon cooling and suppressed by doping, which is in good agreement with the $Ba(Fe_{1-x}Co_x)_2As_2$. Interestingly, the maximal amplitude of the E_g phonon splitting in the sample $x = 0.04$ is very close to the undoped $BaFe_2As_2$.[12] Considering they have similar structural transition temperatures T_s, which characterize the energy scale ($k_B T_s$) of the driving force of the transition, anomalous in-plane phonon splitting in the 122 family might share the same mechanism regardless of the type of the earth-Alcaline, supporting the argument that the FeAs plane control the properties of these systems.[9]

The amplitude of the phonon splitting support a good order parameter to gain some insights into the tetragonal-orthorhombic transition. An order parameter analysis is performed by fitting the temperature dependence of the amplitude of the E_g phonon splitting with $\Delta\omega(T) = \Delta\omega(T = 0\,\mathrm{K}) \times (1 - (T/T_s))^{\beta}$[26] as shown in the Fig. 4. Several tentative values of β ranging from 0.1 to 0.2 produce a set of similar T_s in a good agreement with the structural transition temperature measured in previous study.[19] As a result, the splitting of E_g phonon in $Sr(Fe_{1-x}Co_x)_2As_2$ displays the same temperature and doping dependences as in $Ba(Fe_{1-x}Co_x)_2As_2$, implying universally existed in-plane phonon mode anomalies in the 122 iron-based superconductors.

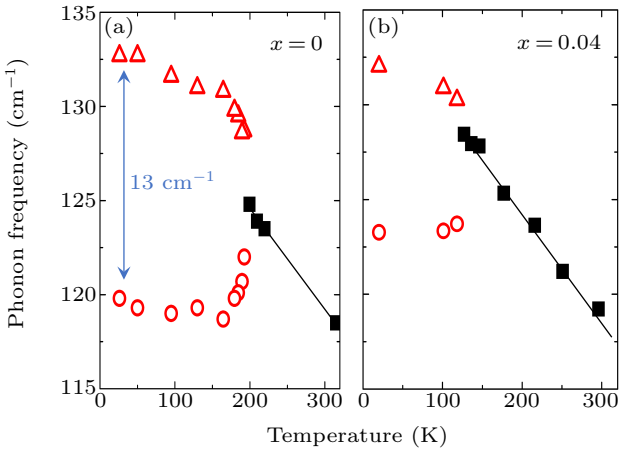


Fig. 3. Evolution of the E_g phonon frequency with temperature for $x = 0$ (a) and $x = 0.04$ (b).

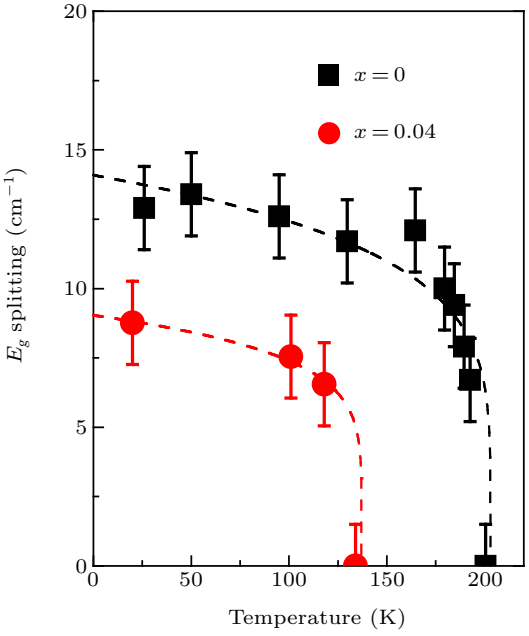


Fig. 4. Evolution of the amplitude of the E_g phonon splitting with temperature for $x = 0$ (black square) and $x = 0.04$ (red circle). The dashed lines are fits using the order-parameter power law described in the text using $\beta = 0.12$.

4. Conclusion

We performed Raman measurements on the $Sr(Fe_{1-x}Co_x)_2As_2$ ($x = 0$ and $x = 0.04$) single crystals. We discovered a large splitting of the E_g phonon modes as the crystals undergo the tetragonal-orthorhombic structural transition, which is similar to what was previously reported for $Ba(Fe_{1-x}Co_x)_2As_2$.[12] As proposed previously, the large splitting cannot simply be driven by the orthorhombic distortion, and strong spin-phonon coupling has been proposed to be a candidate to explain the phonon anomalies. However, we found a much larger maximal amplitude of the splitting in the $Sr(Fe_{1-x}Co_x)_2As_2$ (13 cm^{-1}) than the one in the $Ba(Fe_{1-x}Co_x)_2As_2$ (9 cm^{-1}). Moreover, the sample of $Sr(Fe_{1-x}Co_x)_2As_2$ ($x = 0.04$) displays a similar splitting amplitude and transition temperature as undoped $BaFe_2As_2$, implying the amplitude of the in-plane E_g phonon splitting depends only on the transition temperature, which characterizes the energy scale ($k_B T_s$) of the driven force, regardless of the type of earth-Alcaline. The order parameter analysis exhibits the same doping dependence as reported in the $Ba(Fe_{1-x}Co_x)_2As_2$, implying that the anomalies of the E_g phonon mode might be universal in the 122 family and share the same mechanism.

References

[1] Kamihara Y, Hiramatsu H, Hirano M, Kawamura R, Yanagi H, Kamiya T and Hosono H 2006 *J. Am. Chem. Soc.* **128** 10012

[2] Kamihara Y, Watanabe T, Hirano M and Hosono H 2008 *J. Am. Chem. Soc.* **130** 3296

[3] Takahashi H, Igawa K, Arii K, Kamihara Y, Hirano M and Hosono H 2008 *Nature* **453** 376

[4] Ren Z A, Lu W, Yang J, Yi W, Shen X L, Zheng C, Che G C, Dong X L, Sun L L, Zhou F and Zhao Z X 2008 *Chin. Phys. Lett.* **25** 2215

[5] Wang C, Li L J, Chi S, Zhu Z W, Ren Z, Li Y K, Wang Y T, Lin X, Luo Y K, Jiang S, Xu X F, Cao G H and Xu Z A 2008 *Europhys. Lett.* **83** 67006

[6] Dai Y M, Xu B, Shen B, Xiao H, Lobo R. P. S. M and Qiu X G 2012 *Chin. Phys. B* **21** 077403

[7] Chu C W, Chen F, Gooch M, Guloy A M, Lorenz B, Lv B, Sasmal K, Tang Z J, Tapp J H and Xue Y Y 2009 *Physica C* **469** 326

[8] Mizuguchi Y, Tomioka F, Tsuda S, Yamaguchi T and Takano Y 2008 *Appl. Phys. Lett.* **93** 152505

[9] Mazin I I and Schmalian J 2009 *Physica C* **469** 614

[10] Peng L, Cai C B and Liu Y S 2014 *Chin. Phys. Lett.* **31** 027401

[11] Kang J H, Kim J W, Ryan P J, Xie L, Guo L, Sundahl C, Schad J, Campell N, Collantes Y G, Hellstrom E E, Rzchowski M S and Eom C B 2020 *Proc. Natl. Acad. Sci. USA* **117** 21170

[12] Chauvière L, Gallais Y, Cazayous M, Sacuto A and Méasson M A 2009 *Phys. Rev. B* **80** 094504

[13] Akrap A, Tu J J, Li L J, Cao G H, Xu Z A and Homes C C 2009 *Phys. Rev. B* **80** 180502

[14] Xu B, Dai Y M, Han J, Wang K, Yang R, Yang Y X, Zhang W, Xiao H and Qiu X G 2014 *Physica C* **503** 25

[15] Yang Y X, Gallais Y, Fang Z H, Shi J and Rui X 2015 *Chin. Phys. B* **24** 027401

[16] Yildirim T 2008 *Phys. Rev. Lett.* **101** 057010

[17] Gallais Y, Fernandes R M, Paul I, Chauvière L, Yang Y X, Méasson M A, Cazayous M, Sacuto A, Colson D and Forget A 2013 *Phys. Rev. Lett.* **111** 267001

[18] Yang Y X, Gallais Y, Fernandes R M, Paul I, Chauvière L, Méasson M A, Cazayous M, Sacuto A, Colson D and Forget A 2014 *JPS Conf. Proc.* **3** 015001

[19] Hu R, Bud'ko S L, Straszheim W E and Canfield P C 2011 *Phys. Rev. B* **83** 094520

[20] Ni N, Tillman M E, Yan J Q, Kracher A, Hannahs S T, Bud'ko S L and Canfield 2008 *Phys. Rev. B* **78** 214515

[21] Chu J H, Analytis J G, Kucharczyk C and Fisher I R 2009 *Phys. Rev. B* **79** 014506

[22] Devereaux T P and Hackl R 2007 *Rev. Mod. Phys* **79** 175

[23] Litvinchuk A P, Hadjiev V G, Iliev M N, Lv B, Guloy A M and Chu C W 2008 *Phys. Rev. B* **78** 060503

[24] Martin R M 1970 *Phys. Rev. B* **1** 4005

[25] Jesche A, Caroca-Canales N, Rosner H, Borrmann H, Ormeci A, Kasinathan D, Klauss H H, Luetkens H, Khasanov R, Amato A, Hoser A, Kaneko K, Krellner C and Geibel C 2008 *Phys. Rev. B* **78** 180504

[26] Wilson S D, Yamani Z, Rotundu C R, Freelon B, Bourret-Courchesne E and Birgeneau R J 2009 *Phys. Rev. B* **79** 184519